Pergamon

0734-743X(93)E0003-Z

Int. J. Impact Engng Vol. 15, No. 5, pp. 605–618, 1994
Elsevier Science Ltd
Printed in Great Britain
0734-743X/94 $7.00 + 0.00

A STUDY OF FRAGMENTATION IN THE BALLISTIC IMPACT OF CERAMICS

R. L. WOODWARD,* W. A. GOOCH, JR,† R. G. O'DONNELL,‡
W. J. PERCIBALLI,† B. J. BAXTER* and S. D. PATTIE*

*DSTO Materials Research Laboratory, PO Box 50, Ascot Vale 3032, Victoria, Australia, †US Army Research Laboratory, Aberdeen Proving Ground, Aberdeen, MD, U.S.A. and ‡CSIRO Division of Materials Science, Clayton, Victoria, Australia

(*Received* 4 *May* 1993; *in revised form* 22 *October* 1993)

Summary—Experiments in which both confined and unconfined ceramic targets are perforated by pointed and blunt projectiles are described, and a correlation is established between increased degree of fragmentation and reduced ceramic toughness. Front confinement of the ceramic results in greater overall fragmentation, however fewer, very fine fragments are produced for confined targets compared to unconfined targets. By attributing the fine fragments principally to crushing ahead of the impacting projectile, and coarse fragmentation to the interaction of stress relief waves, the effects of confinement can be qualitatively explained in terms of a simple model for loading and stress relief during perforation. The use of blunt projectiles increases the degree of fragmentation in those cases where the ceramic strength itself is insufficient to fracture the tip on impact. Measurements of fractured ceramic surface area and calculations of fracture work demonstrate that very little of the projectile kinetic energy is consumed in creating new ceramic fracture surface, and it is shown that a high proportion of the projectile impact kinetic energy is redistributed to residual kinetic energy of ejected ceramic debris. For cases where the projectile does not deform during penetration it is possible to derive a value for the average pressure resisting the penetrator. The ballistic efficiency of the ceramic increases with hardness for the lower strength ceramics, however, for the hard ceramics, where the principal influence of the ceramic is to destroy the projectile nose and create an inefficient penetrator, it is found in these tests that the residual penetration depths are similar, and ballistic efficiency is then unrelated to ceramic strength.

1. INTRODUCTION

Ceramic composite armours consist of hard ceramic tiles bonded to ductile backing materials which may be thick or thin, depending on the structural requirements of the armour. Thin backings, which have a thickness in the order of the projectile diameter, pick up momentum, deforming through bending and membrane tension to absorb the residual kinetic energy of the projectile and ceramic fragments. Thick backings show little structural deformation and are perforated by the residual projectile pushing material to the side. The impact face of the armour may be covered with a thin fabric layer to reduce front spall, with little influence on the ballistic performance, or may be covered with a more substantial layer which confines the front face of the ceramic. Ballistic performance may be influenced by the nature and thickness of the ceramic, the confining and backing layers and the geometry of the impacting projectile.

The perforation of a ceramic by a projectile involves penetrator tip fracture and penetrator erosion, loading of the ceramic, ceramic fracture and continued loading of the rubble bed, momentum transfer to, and ejection of, the ceramic debris, and stress wave propagation and interaction within the ceramic and the confining structure. The complexity of these concurrent processes makes it difficult to isolate key parameters which determine performance, measured as resistance to penetration. Previous studies of the interaction between projectiles and ceramic targets have highlighted aspects of modelling [1–5], energy distribution [6–9], ceramic fracture [7–13], and ballistic performance assessment [14–19]. Ceramic fragmentation is important because a large proportion of the projectile kinetic energy is redistributed as kinetic energy of ejected ceramic particles [6–9], however, toughnesses itself is not found to be an indicator of performance [7,10,13].

Fragmentation and ejection of ceramic material are clearly intimately connected to

penetration resistance. As a consequence those properties which may influence fragmentation are investigated in this work, by choosing ceramics with a wide range of toughness and strength, as well as ceramics which have similar measured mechanical and physical properties but which are known to have different ballistic performances. An analysis of the distribution of fragments is performed, and tests of confinement and penetrator geometry effects allow some discussion of the processes of ceramic fracture during penetration. Relationships between ceramic toughness and strength on the one hand and penetration resistance on the other, are explored.

2. EXPERIMENTAL METHODS

The ceramics used included four grades of alumina (prefix AD), two grades of TiB_2, a toughened zirconia and soda lime glass. These materials are listed with their physical and mechanical properties of Table 1. All tiles were 100 mm square and 12.7 mm thick except for the zirconia which was 10 mm thick and the glass which was 15 mm thick.

The tiles were laid up on a backing and surrounded by a close fitting steel jacket to prevent lateral displacement during impact. Two configurations of lay-up were used, referred to as unconfined and confined where the term confinement, in this paper, refers to confinement (or lack of) in the longitudinal direction of the penetrator path. The targets for the ballistic tests were prepared as follows:

Unconfined: Tile bonded to 6.35 thick 2024 T351 aluminium alloy backing plate using a polysulphide adhesive. No front spall shield. Spacing of 150 mm to allow backing plate to deflect, followed by a stack of 38 mm thick 5083 H115 aluminium plates to collect the projectile.

Confined: Tile bonded to a 38 mm thick backing of 5083 H115 aluminium, with successive layers of such plates back to back. Impact side confined by a 6.35 mm 2024 T351 aluminium alloy plate bolted to the steel surround.

Impact in all cases was by a 7.72 mm diameter tungsten alloy projectile. In the pointed configuration the projectile had a slender conical nose (cone angle 30°), was of mass 23.2 g and had a mean impact velocity of 1209 ms^{-1}. In the blunt configuration the projectile had the nose removed to form a flat of diameter 6.6 mm, giving a projectile mass of 19.9 g and mean impact velocity of 1243 ms^{-1}. The target was surrounded by a welded steel catcher box which was sealed except for the hole made by the projectile in a 0.5 mm aluminium disc along the line of projectile flight. The residual depth of penetration into the backing provided an approximate single shot merit assessment.

Following impact, the recovered ceramic debris from the entire tile was sized into fractions by sieving and quantitative metallographic procedures were used to estimate fragment surface areas in each size fraction, for some cases [6]. Data can be presented as mass of

TABLE 1. TILE PHYSICAL AND MECHANICAL PROPERTIES

Ceramic	*Density* ($kg\,m^{-3} \times 10^3$)	*Elastic modulus* (GPa)	*Toughness* K_{1c} ($MPa\,m^{\frac{1}{2}}$)	*Compressive strength* (MPa)	*Hardness (diamond pyramid)* (GPa)
AD85	3.43	224	3.2	2175	8.8
AD90	3.58	268	3.3	2345	10.6
AD96	3.74	310	3.7	2660	12.3
AD995	3.90	383	4.7	2785	15.0
TiB_2 (Ceradyne)	4.52	414	4.1	~5700	27.0
TiB_2 (Cercom)	4.52	538	5.2	~6000	26.1
ZrO_2 (Nilcra, MS)	5.72	205	12.0	1900	11.2
Soda lime glass	2.5	69	0.73	966	5.5

ceramic in each size fraction, or because of the slightly different densities, dividing the mass fractions by ceramic bulk density converts the data into the volume of ceramic debris in each size fraction for direct comparison. The surface area data can be used to obtain the work done in fracturing the ceramic if the material fracture toughness is known. The recovery of fragments is expected to be poorer for the very fine fragments and this effects the volume data shown in the fragment size distribution plots as well as the surface area measurements. The uncertainties in the data are not sufficient to change the general conclusions drawn from the fragment data. Although the whole tile was recovered as fragments, the total volume of fragments would represent the original tile volume and is not a relevant parameter, therefore the data is examined in various size ranges. The original tile surface area was subtracted from the measured total fragment surface area to give the area created in fracture.

3. RESULTS AND DISCUSSION

3.1. *Toughness and fragmentation*

Figure 1 illustrates dramatically the influence large differences in toughness can have on the volume of fragments in any size range of the fragment distribution, by plotting the volume of fragments in a size range against size, for confined targets of (a) glass, (b) AD995 alumina and (c) zirconia. The slightly different thicknesses of the glass and zirconia tiles do not influence the general conclusions to be drawn from this data.

Figure 2 shows cumulative fragment volume against size for the confined and unconfined targets, respectively. These plots indicate a general correlation between an increased volume of fragments produced, and a lower ceramic fracture toughness. However, within the band of results covering those ceramics considered for armour applications (grades of alumina and TiB_2), where toughness ranges from 3.2 to 5.6 MPa $m^{0.5}$, there are contradictions to this general rule, and the ordering of the results also varies with the size range. The use of volume of fragments in any size range allows a more direct comparison between ceramics of different density than the use of the mass of fragments. Repeat shots were performed for AD90, AD995 and zirconia and these results indicate a significant shot to shot variation in the total number of fragments in each size fraction (of the order of 25%). This shot-to-shot variation is a combination of reproducibility of the target construction (particularly degree of confinement), variations in impact conditions, tile to tile variations in ceramic fracture behaviour, and variations in projectile shatter. Both confined shots against AD995 involved negligible yaw and produced similar residual penetrations into the backing (45 and 44 mm) and yet there is a substantial difference in tile fragmentation. The different thicknesses of glass and zirconia tiles can be approximately corrected or in Fig. 2(a) by reducing the former volumes by 16.6% and increasing the latter by 25%. These adjustments do not change the ordering of the results.

To further explore the correlation between degree of fragmentation and toughness, the volume of fragments is plotted against toughness in Fig. 3 for the confined targets, for all fragments less than 0.5 mm and for fragments in the size range 2 to 4 mm. Overall there is a clear inverse relationship which conforms with earlier work [7,10]. The curves in Fig. 3 rely on extreme data points for the very brittle glass and for the very tough zirconia, and a group of points for all the alumina and TiB_2 tiles. This emphasises that the variation in fragmentation behaviour arising from small differences in toughness is masked by the shot-to-shot consistency of results, as is also evident in Fig. 2. The points for AD85 alumina and glass are enclosed in brackets because they are expected to be underestimates as in these cases the impacting projectile did not fracture or deform, as discussed below.

3.2. *Confinement*

A comparison of fragment cumulative volume data for confined and unconfined ceramics of the same ceramic type, Fig. 2, shows that generally more overall fragmentation is produced when the ceramic is confined. Nevertheless, if only the finest groups (<0.18 mm)

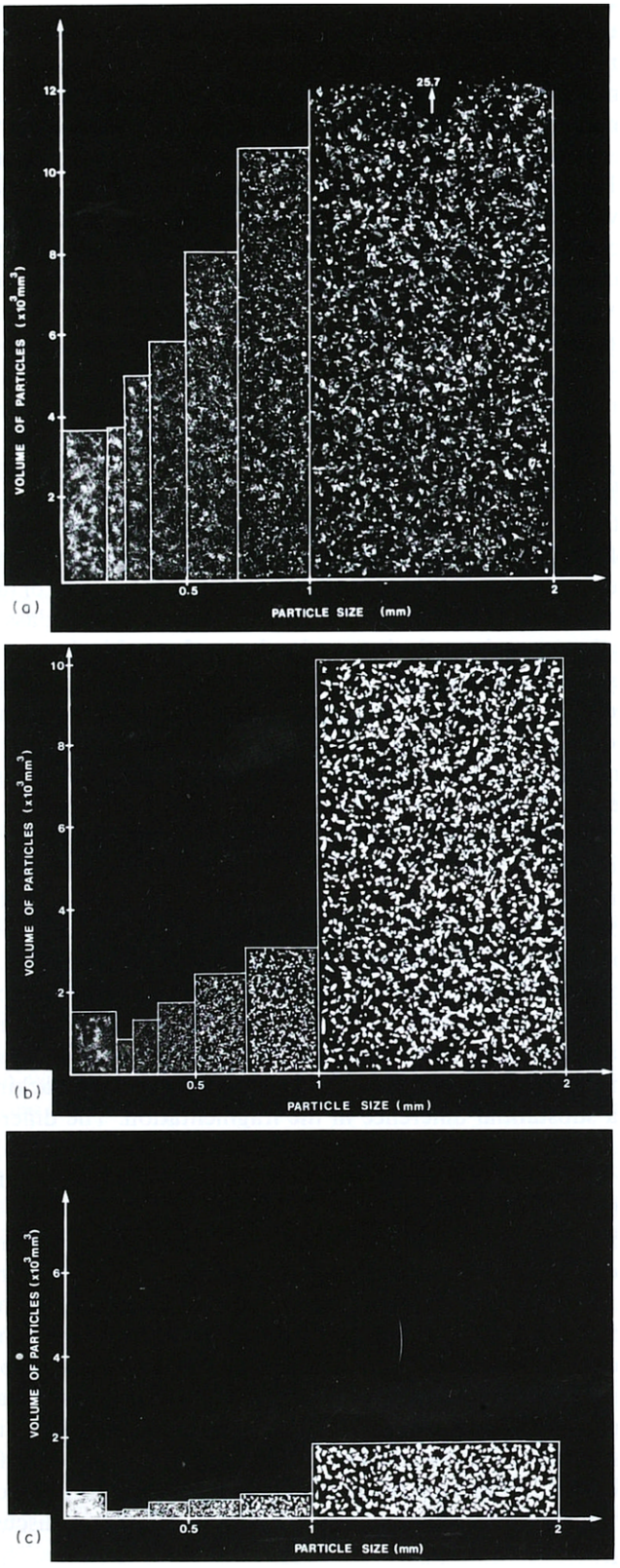

FIG. 1. Volume of fragments against fragment size for confined (a) glass, (b) AD995 alumina and (c) zirconia ceramic targets, impacted by a pointed projectile. The fragment relative sizes are also indicated by the typical fragments in each size fraction. The total volume of the glass tile was 18% greater, and that of the zirconia 27% smaller, than the alumina tile.

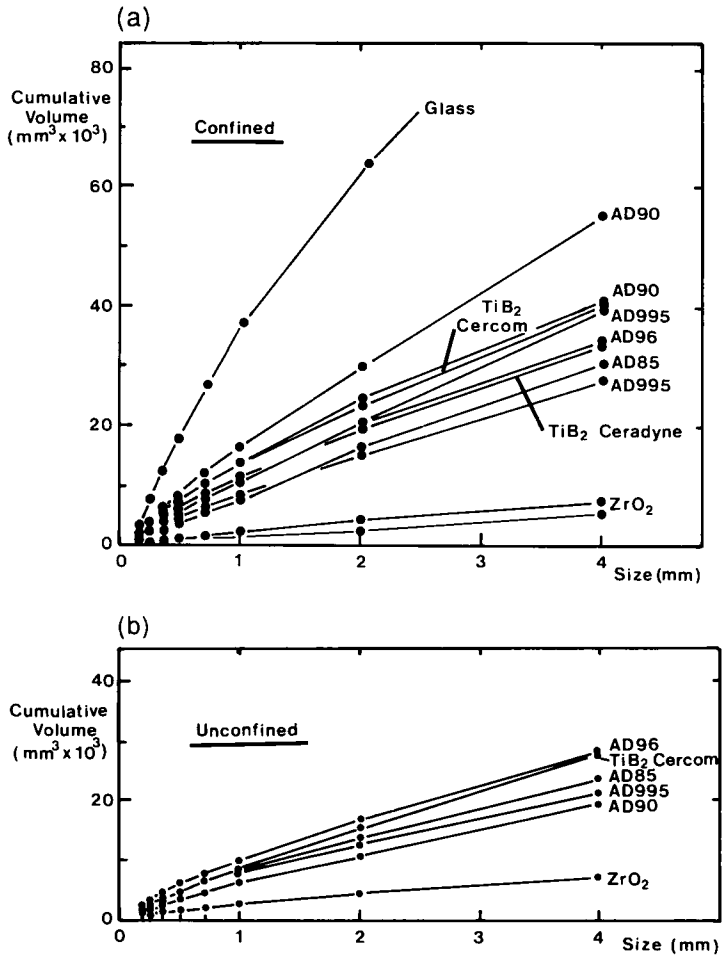

FIG. 2. Cumulative volume of ceramic fragments as a function of maximum fragment dimension in each particle size fraction for (a) confined targets and (b) unconfined target.

of fragments are considered then the unconfined impacts produced more of these "very fine" fragments. Two exceptions for this were AD90 and the Cercom TiB_2. The phenomenon is clearly shown in the comparative volume plots for AD90 alumina of Fig. 4. The sequence of events is qualitatively pictured in Fig. 5 for a confined target impact and in Fig. 6 for an unconfined target impact. In the confined target sequence of Fig. 5, the penetrator moves into and is eroded along with the ceramic, and the ceramic debris is ejected at a high velocity from the crater. A compressive stress wave propagates away from the penetrator, subjecting the whole tile to a hydrostatic pressure, and ceramic is crushed in front of the advancing projectile. This is followed by a relief wave which allows the confining plate to move, relieving the hydrostatic compression and allowing ceramic fracture in an arc below the confining plate. For the unconfined case, Fig. 6, there is no confining plate to move so a relief wave propagates directly into the ceramic allowing easier tensile fracture and ejection of debris away from the crater. At later times, another relief wave reflected from the thin backing allows the backing to move, and further reduces the hydrostatic confinement ahead of the projectile. If we assume the very fine debris arises from crushing ahead of the penetrator, and that the coarser fragmentation arises from stress wave relief cracking away from the crater then the general features of the fragmentation distribution are explicable. Thus, for the confined targets, the higher hydrostatic pressures reduce the amount of fine fragmentation in the crater region; however, higher pressures also result in higher intensity relief waves which produce, as a consequence, more coarse fragmentation away from the crater. This concept for the causes of coarse and fine fragment fractions is

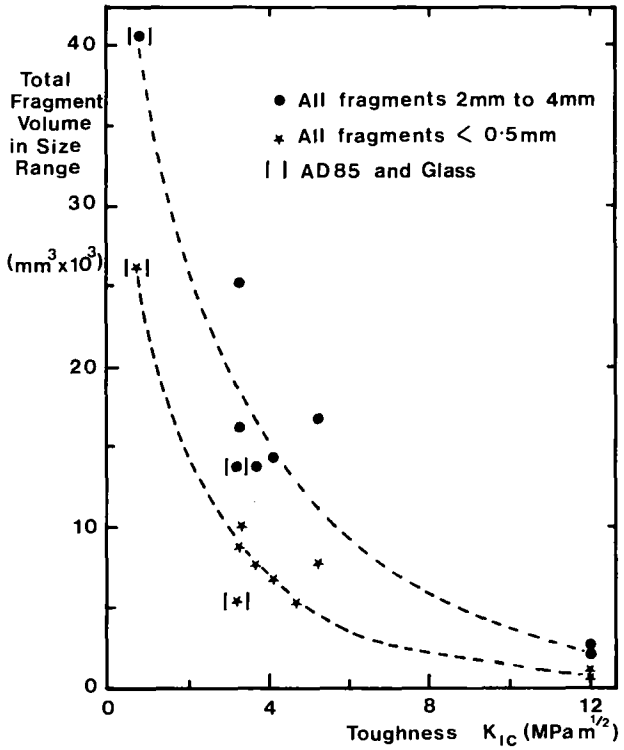

FIG. 3. Total volume of fragments in size fractions <0.5 mm and 2–4 mm, plotted against fracture toughness, K_{Ic}, for the confined ceramic targets.

consistent with the pattern seen on disassembly of the confined targets, Fig. 7, which shows the finest fragments in the centre of a fine fracture region thicker on the impact side of the target.

3.3. *Projectile geometry*

The toughest and the most brittle of the materials were also impacted by flat ended projectiles. The fragment distributions of Fig. 8 can be compared to those for the same materials with a pointed projectile in Fig. 1. There is a large increase in volume of fine fragments when the glass is impacted by a flat ended projectile, Figs 1(a) and 8(a), however within the consistency of the fragmentation data there is effectively no difference between the zirconia data for pointed and blunt projectiles, Figs 1(c) and 8(b). The explanation of this behaviour is based on the premise that the finer fragmentation is produced by crushing ahead of the penetrator. For a pointed projectile impact on the glass the projectile does not deform and the glass is loaded by a tapered section pushing it to the side. With the blunt projectile, of the same material, as well as a higher impact shock pressure, the average pressure during penetration has increased to the extent that the penetrator itself deforms (as was observed in penetration of the glass by the blunt projectile), the higher uniaxial load also producing greater fragmentation ahead of the projectile. For the impact on the zirconia it is found that the tile is sufficiently hard to destroy the tip of the pointed projectile on impact so that impacts with pointed and blunt projectiles are effectively similar. The concepts help explain why the AD85 alumina does not produce as much fragmentation as expected, given that it is the ceramic with the least toughness, Fig. 2. This ceramic was low enough in strength that the penetrating pointed projectile did not deform; as the pointed and blunt firings against glass demonstrate, this leads to much less fragmentation. In all other cases the ceramic strength was sufficient to fracture the nose of the pointed projectile. For this reason the AD85 and glass data points are singled out as under-estimates in Fig. 3.

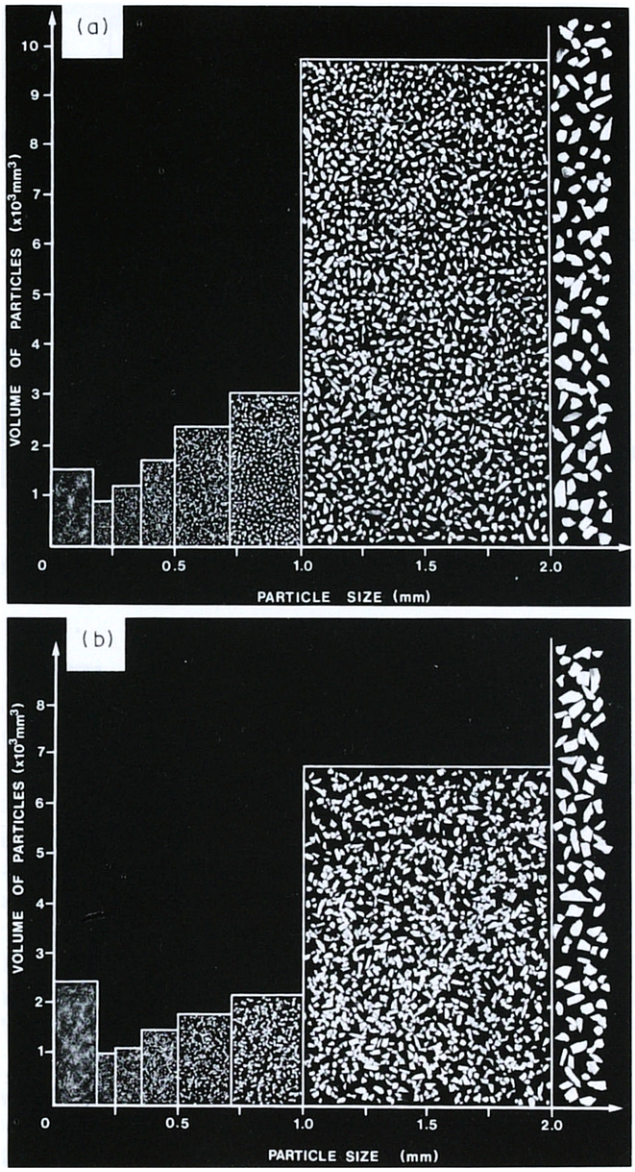

FIG. 4. Fragment volume distributions for pointed projectile impact on AD96 alumina tiles in (a) confined and (b) unconfined configurations.

3.4. *Redistribution of impact kinetic energy*

Table 2 presents data on residual depth of penetration into the backing target (the maximum depth of the penetration crater) for the pointed projectile fired into confined and unconfined alumina targets as well as both total surface area created in fracture of the ceramic and work done in fracturing the ceramic. Figure 9 presents surface area created as a function of particle size, and indicates that most of the surface area is in fragments of dimension less than 1 mm in size. The surface area estimates were made using quantitative steriological methods on each size fraction [7]. By multiplying the total surface area by one half of the fracture toughness or the strain energy release rate, $G(=K^2(1-\nu^2)/E)$, one has a figure for the total work to create this surface.

The impact kinetic energy of the pointed projectile is 16.95 kJ and by comparison the work done in fragmentation of the ceramic, as presented in Table 2, is negligible. The value of strain energy release rate, G, which is the work to produce new surface, includes inelastic

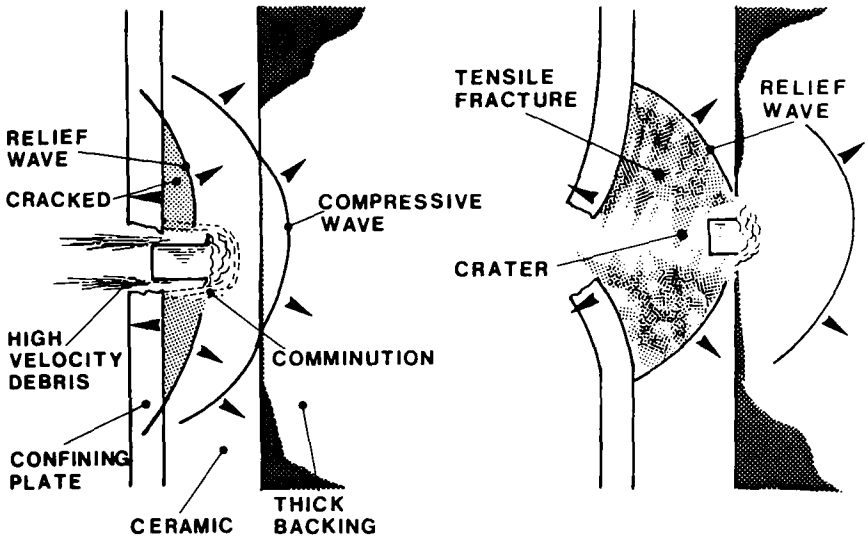

FIG. 5. Schematic representation of the sequence of events following ballistic impact on a ceramic with a confining front plate and a thick backing.

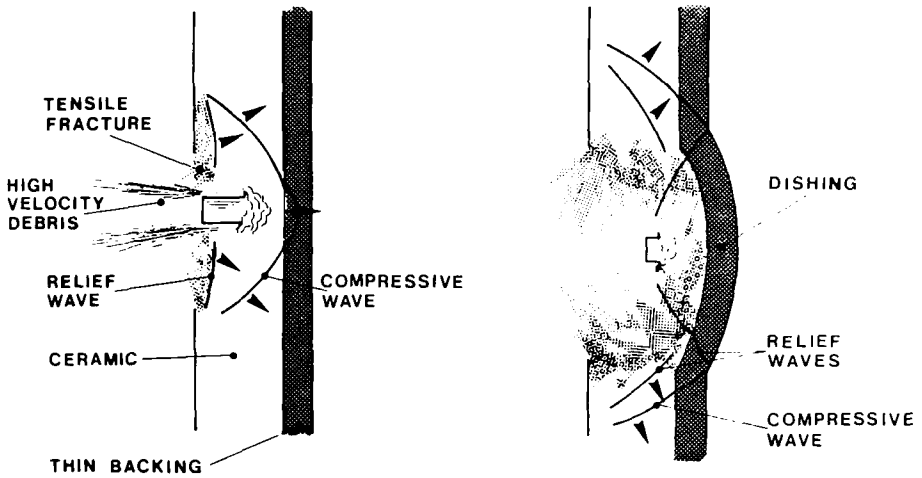

FIG. 6. Schematic representation of the sequence of events following ballistic impact on a ceramic with a thin backing.

processes associated with fracture; any particle–particle interactions producing heat will produce further fracture in such brittle materials and will therefore be counted in such a fragmentation analysis. Furthermore, the use of "dynamic" toughness values and recovery of the maximum 1% missing fragments is not sufficient to change the inescapable conclusion that very little of the projectile's kinetic energy ends up as fracture energy.

Table 2 shows that for the confined AD85 target, the residual path of penetration is 46% of the depth of penetration with no ceramic tile, thus indicating that 54% of the projectile kinetic energy has been removed by some other process, assuming that depth into the aluminium is some way proportional to kinetic energy. This is reasonable for the glass and AD85 cases where the projectile does not deform, and residual penetration of the aluminium by the pointed projectile is by radial flow [20,21]. For the pointed projectile penetrating the glass target the residual depth was 75% of the depth of penetration into the aluminium pack, indicating that the glass has removed approximately 25% of the projectile kinetic energy. Simple plasticity calculations indicate less than 0.5 kJ is necessary to perforate the aluminium confining plate and only 0.4 kJ of work is needed for the 4 mm

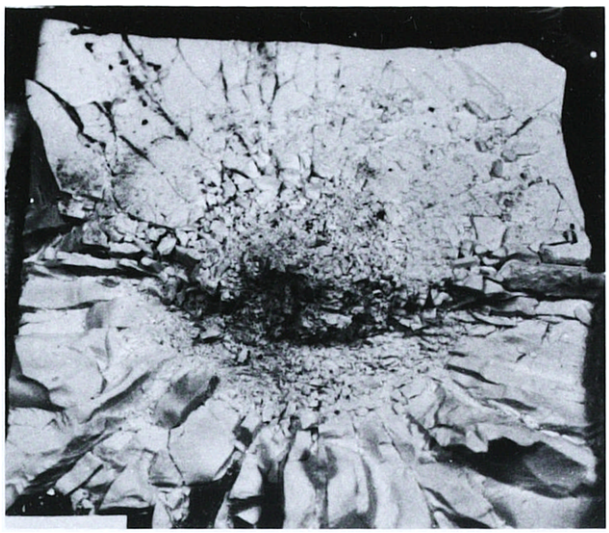

FIG. 7. Post-impact view of fragmented ceramic following removal of the confining plate only and a portion of the ceramic debris.

dishing of the confining plate in the case of the AD85 target. Thus for the AD85 alumina approximately 49% and for the glass approximately 20% of the projectiles initial kinetic energy must still be accounted for. For both AD85 and glass there is negligible projectile deformation, and since we have calculated, above, the negligible amount of energy going into inelastic deformation and fracture of the ceramic, the conclusion is that a large amount of projectile impact kinetic energy is converted into residual kinetic energy of the expelled high velocity ceramic debris. This is consistent with photographic evidence of high velocity debris ejection from the crater for projectile impacts on glass seen in the work of Pavel *et al.* [22], and with studies of geophysical impact cratering phenomena [6].

For all the other cases examined, there was a greater reduction in projectile penetration capability in perforating the ceramics, as indicated by residual depths of penetration. In these cases, the reduction in penetrator effectiveness in perforating the ceramic is partly a consequence of destruction of the penetrator tip as well as plastic deformation of the penetrator and erosive mass loss [19]. Nevertheless, simple estimates of plastic work done on the penetrator and comparison of fractured penetrator performance with blunt penetrator perforation of the aluminium backing [19] still allow the conclusion that momentum transfer to the ceramic and ejection of debris is a principal energy redistribution mechanism [7,9].

3.5. *Penetration resistance*

With the exception of the AD85 alumina, the depth of penetration data given in Table 2 are insufficient to separate the various grades of alumina in terms of penetration resistance, and also insufficient to separate confined versus unconfined targets for penetration resistance. The softer AD85 ceramic performed worse than the others when confined, as it was not able to fracture the projectile. For the unconfined AD85, the projectile fractured, and asymmetric tumbling on exit from the back-up plate resulted in a poor presentation to the pack of aluminium blocks and as a consequence lower than expected residual penetration. The major effect of the ceramic in the present test, whether confined or unconfined, is through blunting the penetrator tip rather than erosive mass loss, and the test (with this projectile and backing) is inappropriate for separating ceramics which are close in performance, especially with the use of a single shot.

A restricted comparison of performance is given in Table 3 where resistance to penetration is defined in terms of a ballistic efficiency parameter, η, defined by Rosenberg and Yesherun

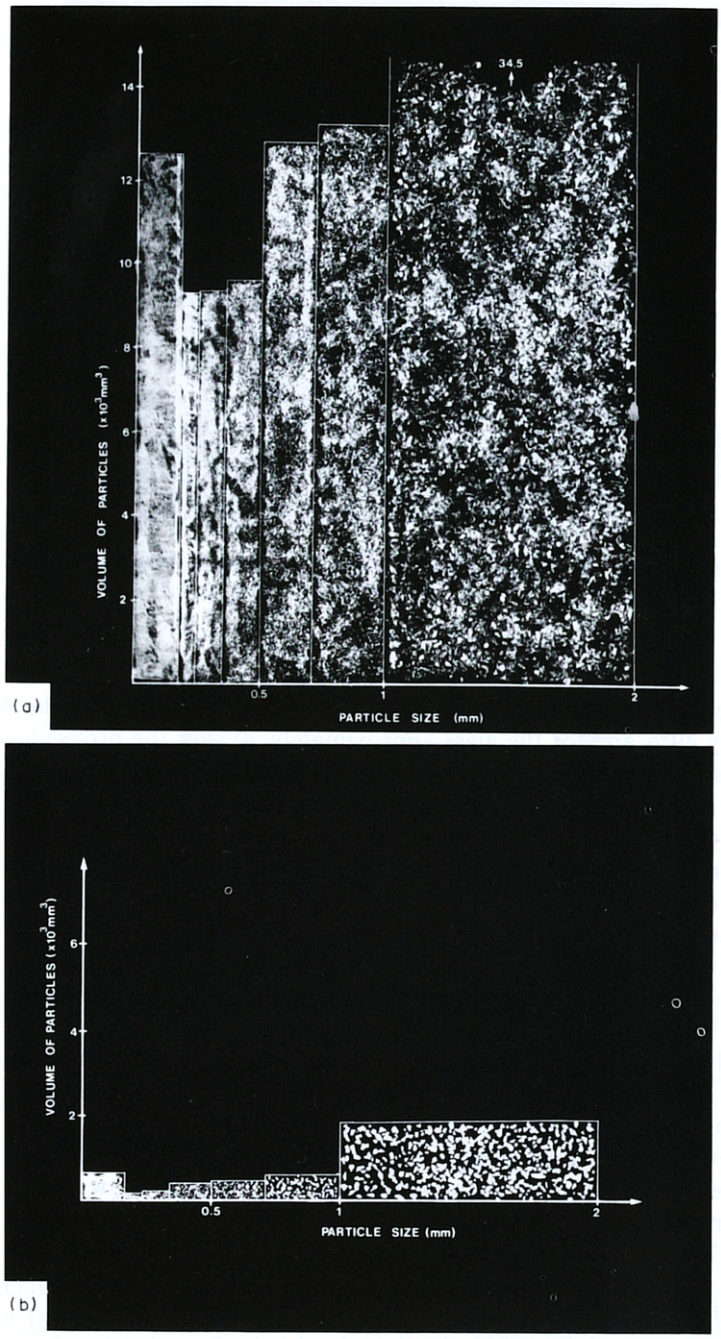

FIG. 8. Volume of fragments as a function of fragment size for confined targets of (a) glass and (b) zirconia, impacted by a blunt projectile.

[16] as

$$\eta = \frac{\rho_{A1}\Delta h_{A1}}{\rho_c h_c} \tag{1}$$

where ρ_{A1} and ρ_c are the densities of aluminium and ceramic, respectively, h_c is the ceramic tile thickness, and Δh_{A1} is the reduction in thickness of aluminium penetrated when the ceramic tile is in place.

From the penetration into aluminium a mean resisting pressure, P_{A1} can be calculated

TABLE 2. RESIDUAL PENETRATION DEPTH, SURFACE AREA AND FRACTURE WORK FOR ALUMINA CERAMICS PERFORATED BY A POINTED PROJECTILE

Ceramic	*Configuration*	*Ceramic areal density* (kg/m^2)	*Residual* penetration depth* (mm)	*Total surface area created* (m^2)	*Total ceramic fracture work* (J)
AD85	Confined	43.6	122.0	0.24	6.2
AD90	Confined	45.9	47.7	0.24	5.1
AD96	Confined	48.0	50.4	0.26	8.6
AD995	Confined	49.7	45.1	0.25	8.8
AD85	Unconfined	43.6	37.1	0.22	5.7
AD90	Unconfined	45.9	63.6	0.11	2.3
AD96	Unconfined	48.0	47.7	0.18	6.1
AD995	Unconfined	49.7	53.0	0.14	5.0

* Depth of penetration into aluminium without ceramic is 265 mm.

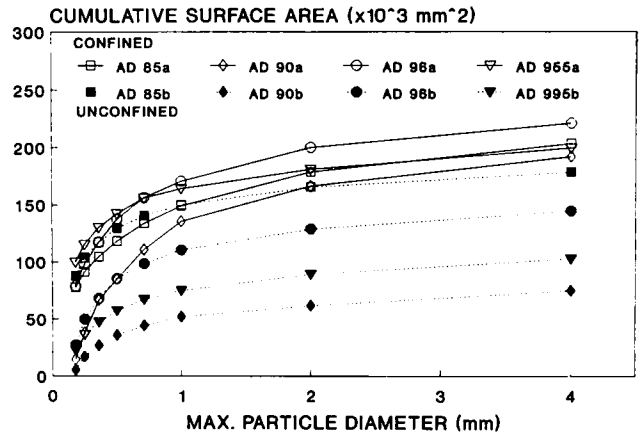

FIG. 9. Plots of cumulative surface area against maximum fragment diameter for the four alumina ceramics in both the confined and unconfined configurations.

TABLE 3. BALLISTIC EFFICIENCY AND PENETRATION RESISTANCE

Material	*Projectile*	*Depth of penetration* (mm)	*Ballistic efficiency* (Eqn 1)* (η)	*Hardness (diamond pyramid)* (GPa)	*Mean P resisting penetration* (GPa)
Aluminium	Pointed	265.0	—	1.03	1.39
Glass	Pointed	200.0	4.2	5.5	5.4
AD85	Pointed	122.0	8.6	8.8	15.2
AD995	Pointed	50.0	11.7	15.0	
Zirconia	Pointed	68.0	9.3	11.2	
TiB_2 (Ceradyne)		38.0	11.1	27.0	
Aluminium	Blunt	75.0	—	1.03	
Glass	Blunt	46.0	1.6	5.5	
Zirconia	Blunt	42.0	1.3	11.2	

* Thin front confining plate ignored in calculations using Eqn 1.

using:

$$\tfrac{1}{2}mv^2 = P_{A1}Ah_{A1} \tag{2}$$

where the first term is the projectile impact kinetic energy (mass, m, and impact velocity, v). Also, A is the presented area of the projectile, and h_{A1} is the depth of penetration into the aluminium block.

Similarly, using this value of P_{A1} a value can also be found for the mean pressure resisting penetration into the ceramic, P_c, using

$$\tfrac{1}{2}mv^2 = P_cAh_c + P_{A1}Ah_{A1}^1 \tag{3}$$

where h_c is the ceramic tile thickness, and h_{A1}^1 is the residual depth of penetration into the aluminium.

The results of these calculations are given in Table 3 for comparison with hardness data (diamond pyramid) and relative ballistic efficiency values for the two cases where the projectile did not deform (AD85 and glass).

It may be anticipated that resistance to penetration by a projectile is related to the material hardness, which is a measure of its resistance to a blunt indenter. Examination of the pointed projectile data in Table 3 for Ballistic Efficiency and Hardness shows a reasonable correlation between the two, except for the case of the Ceradyne TiB_2. The correlation also does not hold for the blunt projectile data where Ballistic Efficiencies are low. If fracture of the ceramic occurs, then pressure resisting penetration may be expected to have a value lower than the material hardness because of the reduced ability of fractured material to support shear stresses. On the other hand the requirement to increase the momentum of the ceramic material which is being rapidly displaced or ejected may increase this resistance to penetration in proportion to the impact velocity. The pressure with which the aluminium resists penetration by the pointed projectile is of similar magnitude to its hardness. The mean resistance provided by the glass is also similar to the hardness, however, in this case this is surprising because fracture would be expected to reduce the effective strength of the glass. Whilst the value of 5.4 GPa in Table 3 for glass is expected to be made up of a component overcoming the material strength and a component to increase the momentum of the glass, the magnitude of the individual contributions is uncertain. Pavel *et al.* [22] present data for penetration of thick glass specimens by a non-deforming projectile at 1060 ms^{-1} and analysis of this data indicates an average resisting pressure of the order of 1.2 GPa, although numerical studies by Pavel *et al.* [22] showed that the actual pressure varies significantly during the event and can be much higher than this average value. The mean resisting pressure for AD85 alumina is much greater than its measured hardness. For the three hardest ceramics against the pointed projectile, Table 3, the reduction in penetration depth is largely due to the ability of these ceramics to blunt the projectile making it an inefficient penetrator, as indicated by the effect of blunting on depth of penetration into bare aluminium. Thus these ceramics have similar ballistic efficiencies, independent of hardness. For cases where blunt penetrators are used the reduction in penetration is a measure of penetrator velocity reduction and erosive mass loss whilst going through the ceramic, and in this case there is also no correlation with hardness. The low ballistic efficiencies, compared with the pointed projectile case, are largely a consequence of the effect of blunting on the base penetration into the aluminium [19]. At the impact velocities used, the blunt tungsten penetrator deforms even on impact with the aluminium target.

In penetrating the ceramic the projectile does work overcoming the strength of the material, and also in increasing the velocity of the ceramic in order to displace it. If the impact pressure is sufficiently high then plastic deformation of the projectile also accounts for some of the work done. If the target was a metal then the work done in overcoming the strength of the material would appear principally as distortional strain energy and heat in proportions of approximately 5% and 95%, respectively. Despite the high stress

levels, the strains are small in brittle materials so that the conversion of work to heat cannot account for the work done on a brittle ceramic target. Previous studies [6,7,9] have concluded, on the basis of measured surface areas and fracture work, that the work of fracture is also insufficient to account for the work done in penetration of such a target. A reasonable hypothesis is that by elastic and shock wave reflections and interactions within the fragmenting material, the work done in overcoming the material strength also contributes to the increase in kinetic energy of the ceramic debris. This relationship of penetration resistance to momentum transfer may partially explain the difficulty in obtaining a unique number related to material strength which indicates resistance to penetration, and the observed experiment dependence of measures of ceramic penetration resistance [23].

4. CONCLUSIONS

These experiments have demonstrated:

(a) That increased ceramic toughness results in less fragmentation under similar conditions of ballistic impact.

(b) Ceramic front confinement results in greater overall fragmentation but less fragments being produced at the finer sizes compared with an unconfined target, and this can be explained in terms of the fine fragments being produced by crushing in front of the projectile whilst coarse fragmentation results generally from the interaction of stress relief waves throughout the ceramic tile.

(c) The effect of projectile blunting is to increase the degree of fragmentation for those cases where the pointed projectile does not deform in perforating the ceramic, but blunting has a negligible influence in cases where the ceramic itself is of sufficient hardness to fracture a pointed projectile tip on impact.

(d) A negligible proportion of the impact kinetic energy is converted into surface energy of the crushed ceramic.

(e) A large proportion of the projectile impact kinetic energy ends up as kinetic energy of ejected ceramic debris.

(f) A value of average pressure resisting penetration, derived for cases where the projectile remained undeformed during penetration, is not simply related to a ceramic strength value.

(g) For "soft" ceramics, where the projectile remains undeformed, the ballistic efficiency increases with ceramic strength, however, for hard ceramics, where the principal influence of the ceramic is to break the penetrator nose and create an inefficient penetrator, residual penetration depths are similar and ballistic efficiency is not simply related to ceramic strength.

REFERENCES

1. M. L. WILKINS, Mechanics of penetration and perforation. *Int. J. Engng Sci.* **16**, 793–807 (1978).
2. M. L. WILKINS, C. F. CLINE and C. A. HONDEL, Fourth progress report on light armour program. Report UCRL-50694 Livermore: Lawrence Radiation Laboratory, Univ of California (1969).
3. M. L. WILKINS, Computer simulation of penetration phenomena. In *Ballistic Materials and Penetration Mechanics* (Edited by R. C. LAIBLE), pp. 225–252. Elsevier Sci. Pub. Co. (1980).
4. R. L. WOODWARD, A simple one-dimensional approach to modelling ceramic composite armour defeat. *Int. J. Impact Engng* **9**, 455–474 (1990).
5. P. C. DEN REIJER, Impact on Ceramic Faced Armour. Doctoral Thesis, Delft University of Technology, The Netherlands (November 1991).
6. D. E. GAULT and E. D. HEITOWIT, The partition of energy for hypervelocity impact craters formed in rock. *Proc. of 6th Symposium on Hypervelocity Impact*, Vol. II, Part 2, 419–456 (1963).
7. R. L. WOODWARD, R. G. O'DONNELL, B. J. BAXTER, B. NICOL and S. D. PATTIE, Energy absorption in the failure of ceramic composite armours. *Materials Forum* **13**, 174–181 (1989).
8. R. L. WOODWARD, B. J. BAXTER, S. D. PATTIE and P. MCCARTHY, Impact fragmentation of brittle materials. *Dymat 91, 3rd Int. Conference on Mechanical and Physical Behaviour of Materials Under Dynamic Loading*, Strasbourg, *Jnl de Physique IV, Colloque C3* (1991).
9. R. G. O'DONNELL, R. L. WOODWARD, W. A. GOOCH, JR and W. J. PERCIBALLI, Fragmentation of alumina

in ballistic impact as a function of frade and confinement. *Proc 12th Int. Symp. on Ballistics, ADPA*, San Antonio, Texas, U.S.A. Vol. 1, pp. 410–418 (October–November 1990).
10. R. G. O'DONNELL, An investigation of the fragmentation of impacted ceramics. *J. Mats Sci. Letters* **10**, 685–688 (1991).
11. C. TRACEY, M. SLAVIN and D. VIECHNICKI, Ceramic fracture during ballistic impact. In *Advances in Ceramics, Vol. 22: Fractography of Glasses and Ceramics*, Amer. Ceram. Soc. pp. 295–305 (1988).
12. F. LONGY and J. CAGNOUX, Plasticity and microcracking in shock-loaded alumina. *J. Amer. Ceram. Soc.* **72**, 971–979 (1989).
13. W. A. GOOCH, JR, W. J. PERCIBALLI, R. G. O'DONNELL, R. L. WOODWARD and B, J. BAXTER, Effects of ceramic type on fragmentation behaviour during ballistic impact. *Proc. 13th Int. Symp. on Ballistics, ADPA*, Stockholm, Sweden, Vol. 3, pp. 93–100 (June 1992).
14. P. WOOLSEY, Ceramic materials screening by residual penetration ballistic testing. *Proc. 13th Int. Symp. on Ballistics, ADPA*, Stockholm Sweden, Vol. 3, pp. 109–116 (June 1992).
15. Z. ROSENBERG and Y. YESHERUN, An empirical relation between the ballistic efficiency of ceramic tiles and their effective compressive strength. *Proc. 10th Int. Symp. on Ballistics, ADPA*, San Diego, CA, U.S.A. (1987).
16. Z. ROSENBERG and Y. YESHERUN, The relation between ballistic efficiency and compressive strength of ceramic tiles. *Int. J. Impact Engng* **7**, 357–362 (1988).
17. Z. ROSENBERG, Y. YESHERUN and J. TSALIAH, More on the thick backing screening technique for ceramic tiles against AP projectiles. *Proc. 12th Int. Symp. on Ballistics, ADPA*, San Antonio, Texas, U.S.A. 197–201 (October–November 1990).
18. S. J. BLESS, Z. ROSENBERG and B. YOON, Hypervelocity impact on ceramics. *Int. J. Impact Engng* **5**, 165–171 (1987).
19. R. L. WOODWARD and B. J. BAXTER, Ballistic evaluation of ceramics: influence of test conditions. *Int. J. Impact Engng*, in press (1994).
20. G. I. TAYLOR, The formation and enlargement of a circular hole in a thin plastic sheet. *J. Mech. Appl. Math.* **1**, 103–124 (1948).
21. R. L. WOODWARD, The penetration of metal targets by conical projectiles. *Int. J. Mech. Sci.* **18**, 119–127 (1976).
22. W. PAVEL, H. J. RAATSCHEN, R. SCHWARZ, H. SENF and H. ROTHENHAUSLER, Experimental and numerical investigations of the failure behaviour of glass targets under impact loading by rigid projectiles. *Proc. 10th Int. Symp. on Ballistics, ADPA*, San Diego, California (1987).
23. G. E. HAUVER, P. H. NETHERWOOD, R. BENCK, W. A. GOOCH, W. J. PERCIBALLI and M. S. BURKINS, Variation of target resistance during long-rod penetration into ceramics. *Proc. 13th Int. Symp. on Ballistics, ADPA*, Stockholm, Sweden, Vol. 3, 257–264 (June 1992).